Evaluation of Grid-based Uncertainty Propagation for Collaborative Self-Calibration in Indoor Positioning Systems

Andrea Jung[®], Paul Schwarzbach[®], Oliver Michler[®]

Abstract—Radio-based localization systems conventionally require stationary reference points (e.g. anchors) with precisely surveyed positions, making deployment time-consuming and costly. This paper presents an empirical evaluation of collaborative self-calibration for Ultra-Wideband (UWB) networks, extending a discrete Bayesian approach based on grid-based uncertainty propagation. The enhanced algorithm reduces measurement availability requirements while maintaining positioning accuracy through probabilistic state estimation. We validate the approach using real-world data from controlled indoor UWB network experiments with 12 nodes in a static environment. Experimental evaluation demonstrates 0.28 m mean ranging error under lineof-sight conditions and 1.11 m overall ranging error across mixed propagation scenarios, achieving sub-meter positioning accuracy. Results demonstrate the algorithm's robustness to measurement noise and partial connectivity scenarios typical in industrial deployments. The findings contribute to automated UWB network initialization for indoor positioning applications, reducing infrastructure dependency compared to manual anchor calibration procedures.

Index Terms—Auto-positioning, Markov Localization, Ultra-Wideband (UWB), Radio-based Localization, Wireless Sensor Network (WSN), Bayes Filter

I. INTRODUCTION

OCATION-AWARE systems in intelligent transportation, smart cities, and logistics require sub-decimeter positioning accuracy for autonomous navigation, asset tracking, and human-machine interaction [1]. Traditional radio-based localization relies on stationary anchors with precisely surveyed positions, creating deployment complexity that scales superlinearly with network density. Manual anchor calibration represents a substantial percentage of system installation costs [2]. Collaborative networks intensify this challenge through systematic error propagation. Positioning errors create correlated uncertainties that compound throughout the system.

Collaborative self-calibration addresses these limitations by estimating node positions without a-priori knowledge of network topology [3]. However, parametric methods demonstrate critical limitations when addressing non-Gaussian distributions and multimodal uncertainties prevalent in non-line-of-sight (NLOS) environments [2]. Recent surveys identify inadequate

Manuscript received xx xxxxxx 202x; revised xx xxxxxx 202x; accepted xx xxxxxx 202x. Date of publication xx xxxxxx 202x.

Corresponding author: Paul Schwarzbach

Digital Object Identifier ...

The authors are with the Institute of Traffic Telematics, TUD Dresden University of Technology, 01069 Dresden, Germany (e-mail: firstname.lastname@tu-dresden.de).

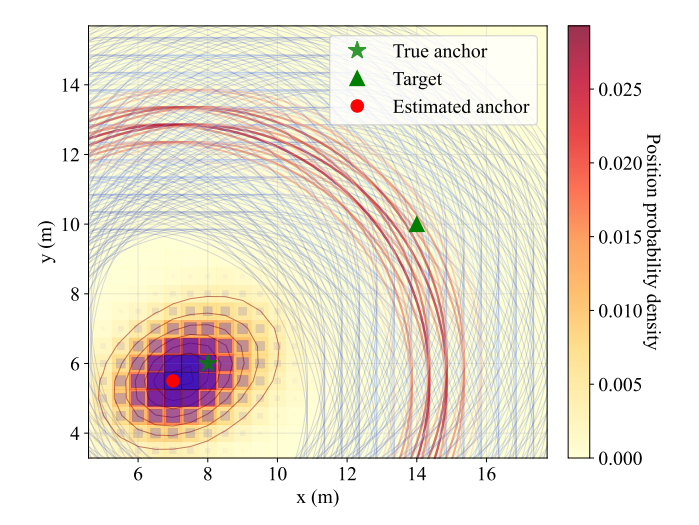


Fig. 1: Grid-based uncertainty propagation for collaborative self-calibration: Anchor probability distribution generates multiple weighted measurement hypotheses (radiating lines) rather than single point-estimate constraints, preserving spatial uncertainty information for robust target localization.

noise models and insufficient uncertainty quantification as fundamental failure modes [1], [4].

This research addresses collaborative self-calibration through probabilistic uncertainty propagation frameworks that achieve sub-meter positioning accuracy while reducing infrastructure dependencies. As illustrated in Fig. 1, the proposed grid-based approach generates multiple weighted measurement hypotheses rather than single point-estimate constraints, preserving spatial uncertainty information for robust target localization. The methodology extends discrete Bayesian estimation to maintain uncertainty distributions across network nodes, validated through experimental evaluation using real-world data from a fully meshed UWB sensor network under mixed propagation conditions. This approach demonstrates superior robustness to initialization parameters and measurement availability constraints compared to conventional parametric methods.

A. Related Work

Collaborative self-calibration encompasses automatic positioning procedures that enable anchor nodes to determine their locations without manual surveying, utilizing peer-topeer ranging measurements [5]. This approach differs from cooperative localization, which focuses on information sharing to improve individual node accuracy [6], by eliminating fixed infrastructure dependencies entirely. The fundamental challenge emerges from uncertainty propagation characteristics in collaborative networks, where positioning errors systematically bias dependent node estimates.

- 1) Collaborative calibration: Collaborative calibration methods enhance accuracy for anchors with approximate known coordinates. Qi et al. [7] address second-order error terms in trilateral localization through tightly coupled UWB-MEMS sensor integration, demonstrating that anchor position errors significantly impact localization performance when neglected in conventional first-order approaches. Xu et al. [8] employ Modified Light Gradient Boosting Models with cooperative screening strategies to handle inhomogeneous estimation errors across diverse network topologies, achieving adaptability across C-shape, H-shape, and O-shape configurations.
- 2) Meshed anchor-tag networks: Technology-specific implementations demonstrate meshed approaches across wireless technologies. WiFi-RTT systems [9] utilize round-trip time measurements for ranging establishment and employ simultaneous localization and mapping (SLAM) approaches, while 5G-based systems [10] leverage combined range and angle-of-arrival measurements to achieve positioning accuracy. UWB-aided vision navigation systems [11] exemplify complementary technology integration for UAV applications. Calibration Unit approaches [12] provide alternative methodologies for inter-anchor distance estimation through dedicated calibration modules with known relative positions.
- 3) Fully meshed networks: Fully meshed approaches achieve network-wide positioning without external references, representing the most autonomous positioning methodologies. Multidimensional Scaling (MDS) approaches form a foundational category, with Krapez et al. [13] demonstrating MDS integration achieving 0.32 m anchor localization accuracy in three-dimensional environments. Closed-form autopositioning approaches [14], [15] provide computational efficiency through direct algebraic solutions, while machine learning enhanced methods [16] achieve centimeter-level accuracy through adaptive physical layer settings and signal correction algorithms.

However, existing parametric collaborative localization methods demonstrate significant limitations when addressing non-Gaussian distributions and multimodal uncertainties prevalent in NLOS propagation environments [2]. Traditional approaches approximate reference position uncertainty through covariance matrices and trace operations [17], effectively discarding spatial distribution structure particularly problematic when reference positions exhibit multimodal distributions. This parametric representation fails to capture true networkwide uncertainty propagation, motivating non-parametric approaches that preserve discrete probability mass distributions throughout collaborative positioning processes.

B. Scope and Contributions

This paper addresses the challenges of collaborative self-calibration in indoor positioning systems by evaluating a grid-based approach in a mixed LOS- and NLOS-environment, where traditional parametric methods exhibit diminished performance due to NLOS propagation and measurement outliers. The primary contributions of this work are threefold:

- We present a self-surveyed dataset acquired from a fully meshed UWB sensor network employing twoway ranging (TWR). This dataset provides empirical validation data for ranging quality assessment in realworld deployment scenarios and captures challenges inherent to NLOS reception and intermittent signal loss.
- 2) We extend and evaluate a previously introduced grid-based Bayesian formulation for collaborative self-calibration [18]. This approach employs non-parametric filtering that preserves uncertainty distributions across network nodes, demonstrating superior robustness compared to parametric self-localization methods. The representation facilitates incorporation of a-priori environmental knowledge to enhance positioning accuracy through informed spatial constraints.
- 3) We demonstrate that the proposed method reduces connectivity requirements and measurement availability constraints compared to state-of-the-art approaches. This reduction enables practical deployment in scenarios where conventional methods fail due to insufficient measurement density or network connectivity limitations. The Bayesian framework ensures consistent positioning performance despite erroneous ranging data typical in NLOS-dominated environments.

The remainder of this paper is structured as follows: Section II establishes theoretical foundations for collaborative self-calibration, introducing a baseline closed-form approach and the novel grid-based approach. Section IV describes the measurement campaign, detailing test scenario configuration and UWB ranging data collection. Section V presents the empirical results, examining ranging performance metrics and comparative positioning performance analysis. The paper concludes with a synthesis of findings and outlook on future research directions in Section VI.

II. FUNDAMENTALS

This section establishes the theoretical foundation for collaborative self-calibration by examining dependency structures in network-based positioning systems and presenting both baseline and proposed approaches. The analysis reveals limitations of conventional parametric uncertainty propagation methods, motivating the main contribution of this research.

A. Collaborative Positioning Dependencies

Collaborative positioning systems exhibit interdependencies that distinguish them from conventional anchor-based localization. Figure 2 illustrates the fundamental dependency structure, where $\mathbf{p}_k^{(i)}$ denotes the position vector of node i at time step k, $z_{ij}^{(k)}$ represents the distance measurement between nodes i and j, and $p(\cdot|\cdot)$ denotes conditional probability distributions.

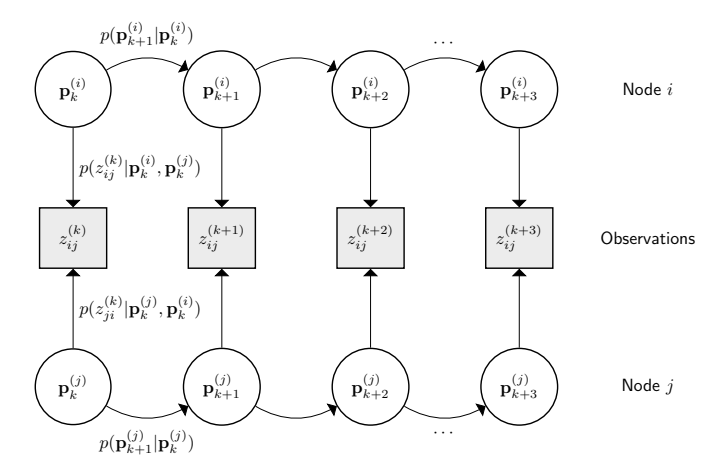


Fig. 2: Dependencies in collaborative positioning networks. Circles denote node states $\mathbf{p}_k^{(i)}$, squares represent observations $z_{ij}^{(k)}$, horizontal arrows indicate temporal evolution $p(\mathbf{p}_{k+1}^{(i)}|\mathbf{p}_k^{(i)})$, and vertical arrows represent measurement dependencies $p(z_{ij}^{(k)}|\mathbf{p}_k^{(i)},\mathbf{p}_k^{(j)})$. This coupling structure creates correlated uncertainties that propagate throughout the network.

Temporal evolution follows prediction models $p(\mathbf{p}_{k+1}^{(i)}|\mathbf{p}_k^{(i)})$ representing positional changes between time steps. The critical challenge emerges from spatial coupling: distance measurements $z_{ij}^{(k)}$ depend simultaneously on both node positions through $p(z_{ij}^{(k)}|\mathbf{p}_k^{(i)},\mathbf{p}_k^{(j)})$. This bidirectional dependency creates systematic bias propagation where positioning errors in individual nodes affect estimates of dependent nodes.

Traditional parametric approaches approximate position uncertainties as additive noise terms, severing the dependency links in Figure 2. This approximation discards distributional information, particularly problematic for non-Gaussian or multimodal uncertainties common in NLOS environments. The resulting estimates become overconfident, failing to capture network-wide uncertainty propagation.

Collaborative systems require estimation methods that preserve and propagate uncertainty information across network nodes while maintaining computational tractability.

B. Baseline Closed-Form Approach

The baseline method, utilizing a fully meshed network as depicted in Fig. 3, establishes a coordinate reference frame using three anchors with the following assumptions [14], [15]:

- a₀ is situated at the coordinate origin
- The direction from a_0 to a_1 defines the positive x-axis
- a₂ lies in the half-plane with positive y-coordinate

The objective is estimating two-dimensional positions $\mathbf{p}_i = [x_i, y_i]^T$ for each node $i \in \{1, ..., N\}$ using the inter-node distance matrix:

$$\mathbf{D}^{(k)} = \begin{pmatrix} z_{0,0}^{(k)} & z_{0,1}^{(k)} & \cdots & z_{0,N}^{(k)} \\ z_{0,0}^{(k)} & z_{1,1}^{(k)} & \cdots & z_{1,N}^{(k)} \\ \vdots & \vdots & \ddots & \vdots \\ z_{0,0}^{(k)} & z_{0,1}^{(k)} & \cdots & z_{0,N}^{(k)} \end{pmatrix}$$
(1)

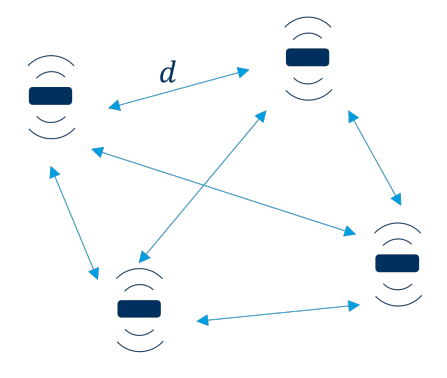


Fig. 3: Fully meshed sensor network configuration

where $z_{ij}^{(k)}$ represents measured distance between nodes i and j at time step k. We distinguish between true geometric distances $d_{ij} = \|\mathbf{p}_i - \mathbf{p}_j\|_2$ and measured distances $z_{ij}^{(k)} = d_{ij} + n_{ij}^{(k)}$, where $n_{ij}^{(k)}$ represents measurement error. The coordinate frame is established by setting $\mathbf{a}_0 = [0,0]^T$

The coordinate frame is established by setting $\mathbf{a}_0 = [0,0]^T$ and $\mathbf{a}_1 = [z_{01}^{(k)},0]^T$. Subsequent nodes are positioned using trilateration:

$$\mathbf{a}_2 = \left[\frac{(z_{02}^{(k)})^2 - (z_{12}^{(k)})^2 + x_1^2}{2x_1}, \sqrt{(z_{02}^{(k)})^2 - x_2^2} \right]^T \tag{2}$$

This approach exhibits several limitations: measurement errors propagate algebraically through squared terms, measurement failures render trilateration infeasible, and the square root operation introduces numerical instabilities when $d_{02}^2 < x_2^2$, motivating the probabilistic approach presented next.

III. BAYESIAN GRID-BASED APPROACH

The key methodological innovation extends the grid-based framework of [18] by implementing hypothesis-based uncertainty propagation rather than parametric approximation of anchor position uncertainties. While parametric approaches collapse probability distributions to covariance matrices, the proposed method preserves and propagates discrete probability mass from anchors, enabling more accurate uncertainty quantification in collaborative positioning scenarios. This is achieved by incorporating weighted contributions from multiple position hypotheses into the likelihood calculation as part of the correction step in a recursive state estimation framework. The overall procedure is summarized in Fig. 4 and detailed in the following.

The approach employs discrete grid representation of the state space, enabling non-parametric probability density estimation that is robust to non-Gaussian measurement noise and multimodal distributions. For each node, the continuous position space is discretized into M equidistant grid points:

$$\mathcal{G} = \{\mathbf{g}_1, \mathbf{g}_2, \dots, \mathbf{g}_M\} \tag{3}$$

The posterior probability distribution over the grid is maintained and updated following Bayes' rule:

posterior
$$\propto$$
 likelihood \times prior (4)

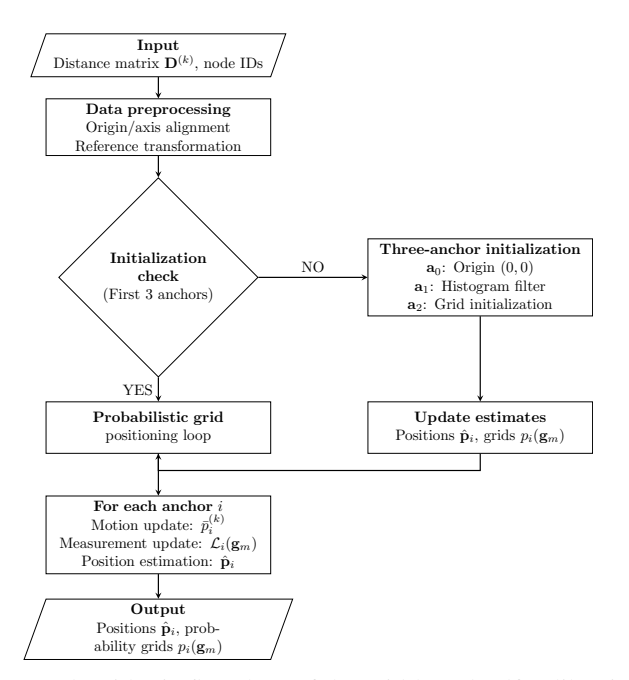


Fig. 4: Algorithmic flowchart of the grid-based self-calibration method. The process implements distance matrix preprocessing, sequential three-anchor initialization (\mathbf{a}_0 at origin, \mathbf{a}_1 via histogram-, \mathbf{a}_2 via grid filter), and recursive Bayesian filtering with uncertainty propagation.

The grid-based approach employs the following parameters:

- M Total number of discretized grid cells
- τ Percentage threshold for probability mass selection
- r_{est} Estimation region radius
- σ_r Ranging measurement standard deviation
- v Expected node velocity (zero for static scenarios)
- σ_v Velocity uncertainty standard deviation

A. Initialization Phase

The proposed method leverages the coordinate frame established in Section II-B while implementing probabilistic estimation. Unlike the deterministic closed-form approach, the initialization phase maintains uncertainty distributions throughout coordinate system establishment.

- 1) Anchor 0 Origin Definition: Following the baseline methodology, the first anchor defines the coordinate system origin $\mathbf{a}_0 = [0,0]^T$. No uncertainty is associated with this mandatory definition.
- 2) Anchor 1 Histogram Filter: The second anchor position is estimated along the positive x-axis using a one-dimensional histogram filter with H hypotheses over the range $[0, d_{\max}]$:

$$p_1(h_j) = \frac{\exp\left(-\frac{(z_{01}^{(k)} - h_j)^2}{2\sigma_r^2}\right)}{\sqrt{2\pi\sigma_r^2}},$$
 (5)

where h_j represent the histogram bins, σ_r denotes the ranging measurement standard deviation, and $d_{\rm max}$ represents the maximum operational range. The position estimation reduces to a one-dimensional problem while maintaining probabilistic uncertainty representation. The non-parametric nature of the

histogram filter enables incorporation of arbitrary probability distributions without restrictive Gaussian assumptions, facilitating robust estimation under multimodal or heavy-tailed measurement error conditions.

3) Anchor 2 - Grid Initialization: The third anchor represents the first implementation of the grid-based uncertainty propagation framework, establishing the foundational probabilistic estimation method applied to all subsequent anchors. Unlike the deterministic origin definition \mathbf{a}_0 and one-dimensional histogram approach \mathbf{a}_1 , \mathbf{a}_2 employs full two-dimensional Bayesian grid estimation. The initialization procedure utilizes three inter-node distance measurements $(z_{01}^{(k)}, z_{02}^{(k)}, z_{12}^{(k)})$ within the grid-based measurement update framework. The trilateration constraints from Section II-B provide geometric initialization of the applicable state space. The grid-based uncertainty propagation processes the three distance measurements through the complete Bayesian framework:

$$p_2(\mathbf{g}_m) = \eta \cdot \prod_{j \in \{0,1\}} \exp\left(-\frac{(\|\mathbf{g}_m - \mathbf{a}_j\| - z_{j2}^{(k)})^2}{2\sigma_r^2}\right)$$
 (6)

where η is the normalization constant ensuring $\sum_{m} p(\mathbf{g}_{m}) = 1$ and \mathbf{a}_{j} denotes the established positions of anchors 0 and 1. The subsequent position estimation $\hat{\mathbf{a}}_{2}$ follows the approach detailed in Section III-B3.

B. Recursive Position Estimation

Following initialization, the remaining anchors employ a recursive Bayesian filter structure, illustrated in Figure 5, following the alternation between prediction and update steps.

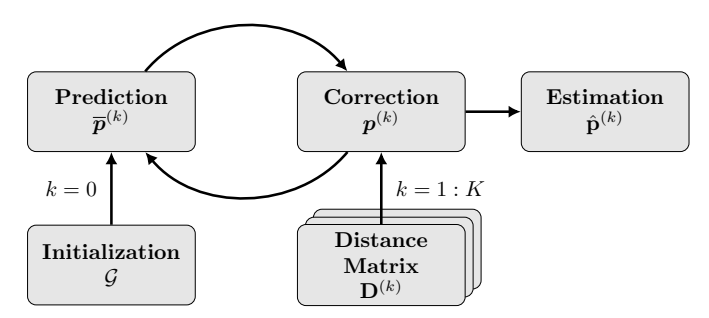


Fig. 5: Recursive filter structure for grid-based self-calibration.

1) Motion Update (Prediction): The prediction step incorporates expected node movement:

$$\bar{p}_i^{(k)} = \sum_{m \in \mathcal{K}} p_m^{(k-1)} \cdot p(\mathbf{g}_i^{(k)} | \mathbf{g}_m^{(k-1)})$$
 (7)

where \mathcal{K} represents the set of grid cells with the highest probabilities. This selection reduces computational complexity while maintaining estimation accuracy. The transition probability is modeled as:

$$p(\mathbf{g}_i^{(k)}|\mathbf{g}_m^{(k-1)}) = \mathcal{N}(\|\mathbf{g}_i - \mathbf{g}_m\|_2 - v\Delta t, \sigma_v^2)$$
(8)

with velocity v and velocity uncertainty σ_v . For static scenarios, v=0 but $\sigma_v>0$ adds noise to enable filter recovery from erroneous estimates.

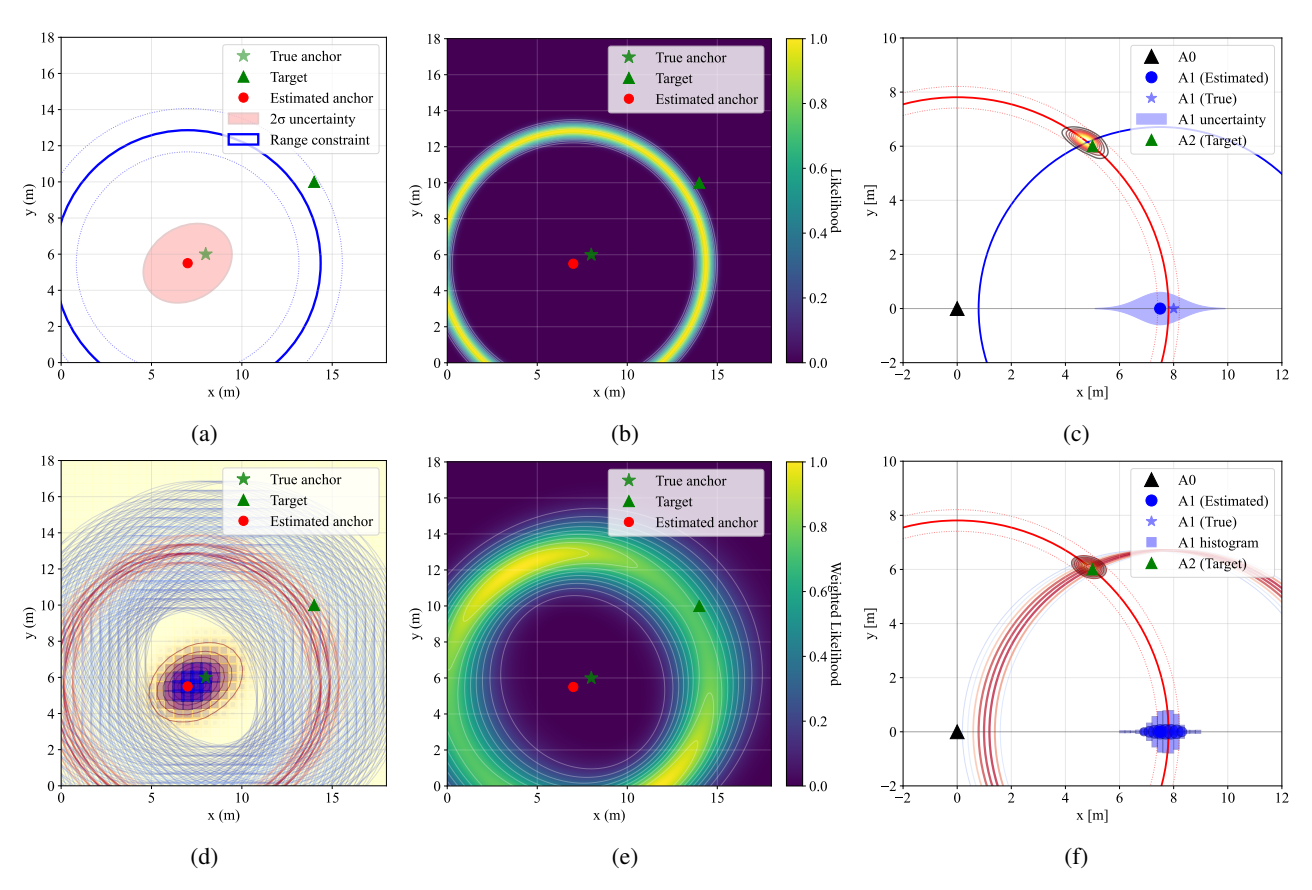


Fig. 6: Uncertainty propagation for collaborative self-calibration: Top row presents traditional point-estimate approach; bottom row demonstrates the proposed grid-based method. (a) Traditional parametric representation of reference anchor as point estimate with associated covariance. (d) Grid-based representation showing probability distribution (colormap), sampled position hypotheses (colored points), and measurement constraints (circles). (b, e) Likelihood computation: (b) single measurement constraint from point estimate; (e) weighted contributions from multiple position hypotheses demonstrating aggregate likelihood fields. (c) Parametric initialization procedure. (f) Grid-based initialization using hypotheses-based uncertainty propagation.

2) Measurement Update with uncertainty propagation: The key methodological innovation addresses uncertainty propagation in collaborative positioning through discrete probability mass preservation rather than parametric approximation. Traditional approaches approximate reference position uncertainty through covariance matrices and apply trace operations [17]:

$$\sigma_{1,2} = \sigma_r + \sqrt{\operatorname{tr}(\mathbf{P}_1)} + \sqrt{\operatorname{tr}(\mathbf{P}_2)} \tag{9}$$

to compute aggregate measurement noise. This parametric representation discards spatial distribution, particularly problematic when positions exhibit multimodal or non-Gaussian distributions common in NLOS-contaminated environments.

The proposed hypotheses-based approach preserves distributional information by maintaining discrete probability mass representations. Rather than collapsing anchor j's position distribution to a single covariance matrix, the method samples the top $\tau\%$ probability mass as discrete hypotheses:

$$\mathcal{T}_j^{\tau} = \{ \mathbf{g}_{jl} : l \in \arg\max_{m} p_j(\mathbf{g}_m) \}$$
 (10)

where each hypothesis retains its associated probability weight $w_{jl} = p_j(\mathbf{g}_{jl}) / \sum_{k \in \mathcal{T}_i^{\tau}} p_j(\mathbf{g}_{jk})$.

For anchor i being updated, the measurement likelihood incorporates uncertainty from all anchors $j \in \mathcal{N}_i$ through weighted contributions from multiple position hypotheses:

$$\mathcal{L}_{i}(\mathbf{g}_{m}) = \prod_{j \in \mathcal{N}_{i}} \sum_{l \in \mathcal{T}_{j}^{\tau}} w_{jl} \cdot \exp\left(-\frac{(\|\mathbf{g}_{m} - \mathbf{g}_{jl}\|_{2} - z_{ij}^{(k)})^{2}}{2\sigma_{r}^{2}}\right)$$
(11)

where:

- \mathcal{N}_i is the set of available reference anchors for node i
- \mathcal{T}_i^{τ} represents the top $\tau\%$ probability cells of anchor j
- w_{jl} are the normalized weights for each hypothesis $z_{ij}^{(k)}$ is the measured distance between nodes i and j at

This weighted superposition captures the true uncertainty propagation from anchors to target positions, as illustrated in Fig. 6. The parametric approximation generates circular measurement constraints from point estimates, while the hypotheses-based method produces aggregate likelihood fields that reflect the actual spatial uncertainty distribution of anchor positions. This distinction becomes increasingly important as positioning errors accumulate through the network.

The posterior probability is updated using Bayes' rule with normalization constant η :

$$p_i(\mathbf{g}_m) = \eta \cdot \bar{p}_i(\mathbf{g}_m) \cdot \mathcal{L}_i(\mathbf{g}_m) \tag{12}$$

3) Position Estimation: The position estimate at each time step is computed as a weighted average in the circular region or radius r around the maximum likelihood estimate with $\mathcal{B}_r(\mathbf{g}_{\text{MLE}}) = \{m : \|\mathbf{g}_m - \mathbf{g}_{\text{MLE}}\|_2 < r\}$:

$$\hat{\mathbf{p}}_i = \frac{\sum_{m \in \mathcal{B}_r(\mathbf{g}_{\text{MLE}})} p_i(\mathbf{g}_m) \cdot \mathbf{g}_m}{\sum_{m \in \mathcal{B}_r(\mathbf{g}_{\text{MLE}})} p_i(\mathbf{g}_m)}.$$
(13)

C. Optional Position Smoothing

To mitigate measurement noise and improve trajectory smoothness, an optional filtering stage can be applied using exponential moving average (EMA) or hybrid median-EMA filtering [19]:

$$\tilde{\mathbf{p}}_i^{(k)} = \alpha \cdot \hat{\mathbf{p}}_i^{(k)} + (1 - \alpha) \cdot \tilde{\mathbf{p}}_i^{(k-1)} \tag{14}$$

where $\alpha \in (0,1]$ is the smoothing parameter.

IV. EXPERIMENTAL SETUP AND DATA COLLECTION

To validate the proposed grid-based positioning method, controlled experiments were conducted in a real-world industrial environment within a business park in Torgau, Germany. The experimental campaign utilized a fully meshed UWB sensor network enabling comprehensive inter-node ranging measurements under mixed propagation conditions.

A. Hardware Configuration

The experimental setup employed 12 Qorvo MDEK1001 UWB transceiver development kits, each comprising DWM1001-DEV development boards operating in the 3.5-6.5 GHz frequency band. The original firmware was customized enable full mesh networking capabilities, supporting simultaneous peer-to-peer ranging between all node pairs. The distance measurements utilized TWR protocol. The network operated with 10 Hz measurement frequency, generating approximately 2.000 measurement epochs. One node served as network coordinator, responsible for communication initialization and centralized data aggregation.

B. Deployment Configuration

A network consisting of 12 nodes were deployed throughout a 44×30 m² indoor hall (see Fig. 7), mounted on tripods at uniform 1.60 m height to ensure consistent measurement conditions. Node positioning was strategically designed to create diverse propagation scenarios, including both LOS and NLOS configurations essential for algorithm robustness evaluation under realistic deployment conditions.

Nodes were powered using USB mains power supplies or USB battery packs, enabling flexible placement without dependency on fixed power outlets. The sensor network was configured and controlled via PC interface, providing access to sensor data and network parameters.

Visibility conditions between node pairs were systematically documented, creating a binary LOS/NLOS classification matrix used for subsequent propagation-dependent analysis.



Fig. 7: Measurement environment with distributed nodes (red) and total station setup for ground truth position surveying.

C. Ground Truth Collection and Reference System

Reference coordinates were established using an optical Leica TS16 total station [20]. A surveying prism, mounted on a tripod together with each node whose position required referencing, served as the target for tachymeter measurements (see Fig. 7). The total station recorded precise coordinates of the prism, enabling creation of a local coordinate system based on predefined reference points in the environment. For compatibility with the proposed algorithm, a coordinate transformation involving both translation and rotation was implemented. In this transformation, two selected nodes define the positive x-axis, with the first node positioned at the coordinate system origin, consistent with the assumptions described in Section II-B. The outcome of this coordinate transformation is illustrated in Fig. 8, demonstrating two distinct node configurations that enable evaluation of anchor initialization sensitivity.

D. Dataset Characteristics

The experimental campaign generated approximately 132,000 individual ranging measurements across all node pairs over 2,000 measurement epochs, providing comprehensive statistical validation data. Each measurement epoch captured the complete 12×12 distance matrix with systematic documentation of ranging availability and residuals.

Data are structured in text format with event timestamps, node identifiers and symmetric distance matrices. The dataset encompasses ground truth coordinates, inter-node ranging measurements, and binary visibility condition matrices for each node pair. Two distinct anchor initialization configurations enable systematic evaluation of algorithm sensitivity to reference frame selection, as illustrated in Fig. 8.

The comprehensive dataset enables robust validation of collaborative self-calibration methodologies under realistic indoor propagation conditions, supporting reproducible performance assessment across varying measurement availability and propagation scenarios typical of industrial deployments.

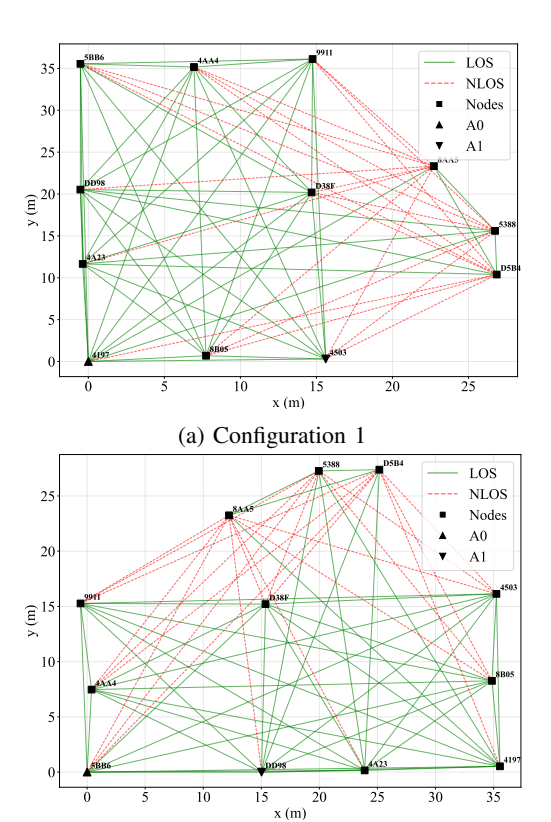


Fig. 8: Node constellation and visibility conditions for both experimental configurations.

(b) Configuration 2

V. VALIDATION AND RESULTS

This section presents validation of the proposed grid-based positioning method using real-world experimental data from the measurement campaign described in Section IV. The evaluation methodology systematically analyzes ranging performance characteristics before comparing positioning accuracy between the baseline closed-form (CF) approach and the proposed probabilistic grid-based positioning (PGP) method across two distinct anchor initialization configurations.

A. Ranging Performance Analysis

The ranging performance evaluation utilizes the complete dataset of 132,000 individual measurements from 12 UWB nodes deployed according to Fig. 8. Statistical analysis is categorized by propagation conditions (LOS/NLOS) to quantify measurement quality variations that directly impact collaborative positioning performance.

Table I presents comprehensive ranging accuracy statistics across propagation conditions. LOS measurements achieve RMSE of $0.28\,\mathrm{m}$ with $0.21\,\mathrm{m}$ median error, exhibiting near-Gaussian error characteristics. NLOS conditions demonstrate significantly degraded performance with RMSE of $3.78\,\mathrm{m}$, reflecting multipath propagation and signal obstruction effects. The combined dataset yields overall RMSE of $1.11\,\mathrm{m}$ with variance $\sigma^2=13.26\,\mathrm{m}$, indicating substantial measurement heterogeneity across the network.

TABLE I: Ranging performance statistics.

Metric	LOS (76.3 %)	NLOS (23.7 %)	Overall (100 %)
Descriptive statistics			
Mean μ (m)	0.28	3.78	1.11
Median (m)	0.21	0.69	0.25
Variance σ^2 (m)	1.59	41.56	13.26
Quantiles			
1σ (m)	0.26	1.41	0.35
2σ (m)	0.47	23.21	5.07
3σ (m)	0.73	24.24	23.63
Percentiles			
25th	0.16	0.54	0.18
50th	0.21	0.69	0.25
75th	0.29	3.79	0.44

Distributional characteristics (Fig. 9) reveal distinct differences between propagation conditions. LOS measurements (Fig. 9a) demonstrate centered, approximately Gaussian distributions. NLOS measurements (Fig. 9b) exhibit heavy-tailed, positively biased distributions with outliers exceeding 20 m.

System-level validation (Fig. 11) confirms measurement consistency despite outlier presence. The quantile-quantile analysis (Fig. 11a) demonstrates linear correlation ($R^2=0.87$) between reference and measured distances across the operational range. The pairwise RMSE matrix (Fig. 11b) reveals systematic measurement quality variations: sensors D5B4, 8AA5 and 9911 exhibit consistently elevated error rates (exceeding 17 m RMSE), correlating with NLOS-dominated node positions in the network constellation (cf. Fig. 8).

B. Measurement Availability Analysis

The availability analysis (Fig. 10) quantifies CF method sensitivity to anchor selection through positioning success rates. Sensor D5B4 demonstrates extreme initialization dependency, achieving zero positioning availability in Configuration 1 which is due to the missing range to sensor 4503 (cf. Fig. 11b), representing a1, as one anchor in the trilateration. In Configuration 2, however, it recovers to an availability of 55.1%. Similarly, sensors 4197 and 8AA5 experience availability variations from 99.8% to 2.9% and 74.6% to 2.8% respectively between configurations.

These variations result from geometric constraints in the CF trilateration process when insufficient measurement connectivity occurs between the established reference frame and target nodes. The CF method requires specific connectivity patterns between the first two anchors and subsequent nodes, creating systematic failure modes when geometric prerequisites are not satisfied.

Cross-referencing with ranging residual analysis (Fig. 11b) reveals that positioning failures do not correspond directly to measurement quality degradation. Sensor D5B4 maintains functional ranging capabilities with multiple network nodes despite elevated error rates with specific pairs (8B05, 9911). The CF method's inability to exploit alternative measurement pathways demonstrates algorithmic rigidity under heterogeneous measurement conditions.

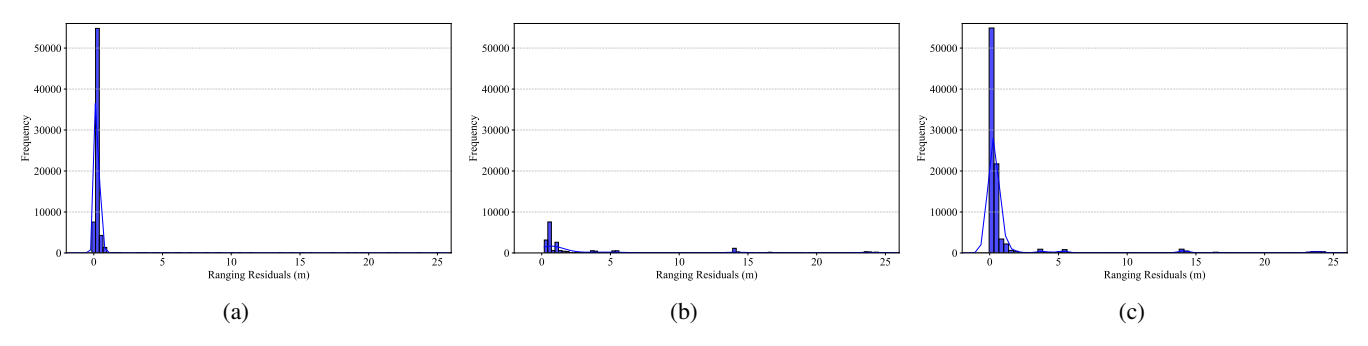


Fig. 9: Ranging residual distributions: (a) LOS conditions showing near-Gaussian characteristics, (b) NLOS conditions exhibiting heavy-tailed, positively biased distribution, and (c) combined dataset demonstrating measurement heterogeneity.

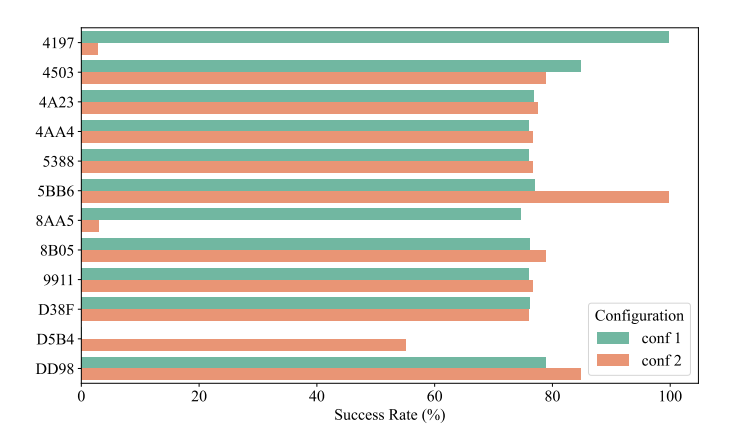


Fig. 10: Measurement availability analysis for CF method across configurations, showing dependency on anchor initialization for individual sensor positioning success rates.

This availability dependency structure presents fundamental limitations for collaborative self-calibration deployments. The deterministic relationship between anchor selection and network-wide positioning success undermines autonomous deployment objectives by requiring a-priori knowledge of optimal initialization configurations. Such requirements effectively transfer calibration complexity from physical surveying to algorithmic parameter selection, contradicting the scalability advantages that collaborative approaches seek to provide.

The observed failure modes highlight the necessity for positioning methods that maintain functionality across varying anchor selections while accommodating the non-Gaussian measurement distributions documented in Section V-A. Probabilistic frameworks that propagate uncertainty distributions rather than point estimates address these geometric constraints through flexible measurement integration approaches.

C. Positioning Performance Comparison

Positioning performance evaluation compares the CF baseline against the proposed PGP method using identical measurement datasets across two anchor initialization configurations (Fig. 8). This methodology isolates anchor selection effects on network positioning accuracy while maintaining consistent environmental and measurement conditions.

Performance distributions (Fig. 12, Fig. 13) reveal fundamental methodological differences. The CF approach exhibits

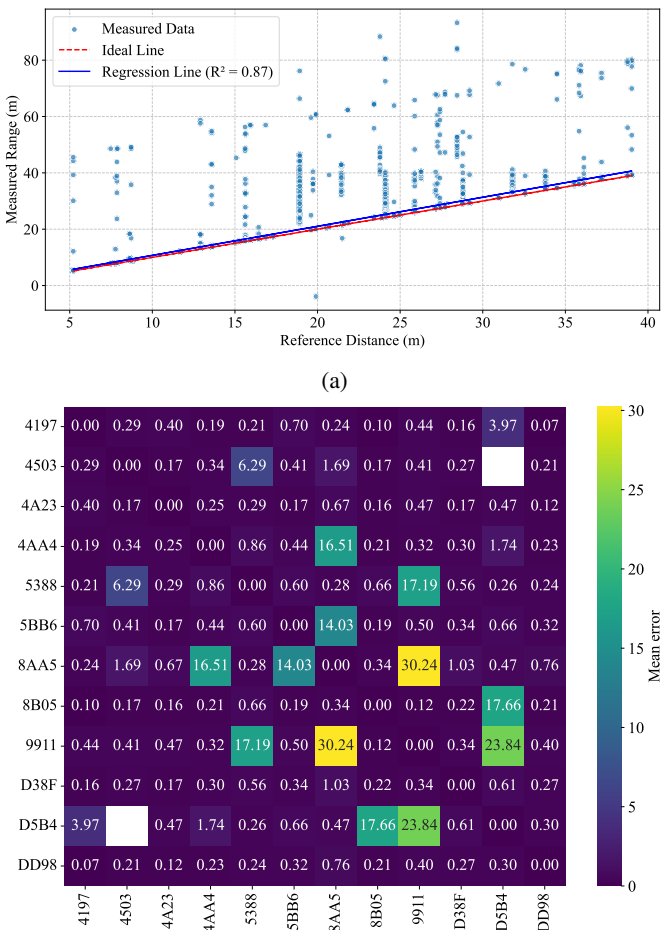


Fig. 11: Ranging accuracy validation: (a) Quantile-quantile plot demonstrating linear correlation ($R^2 = 0.87$) between reference and measured distances, and (b) pairwise RMSE matrix revealing spatial dependencies in measurement quality.

(b)

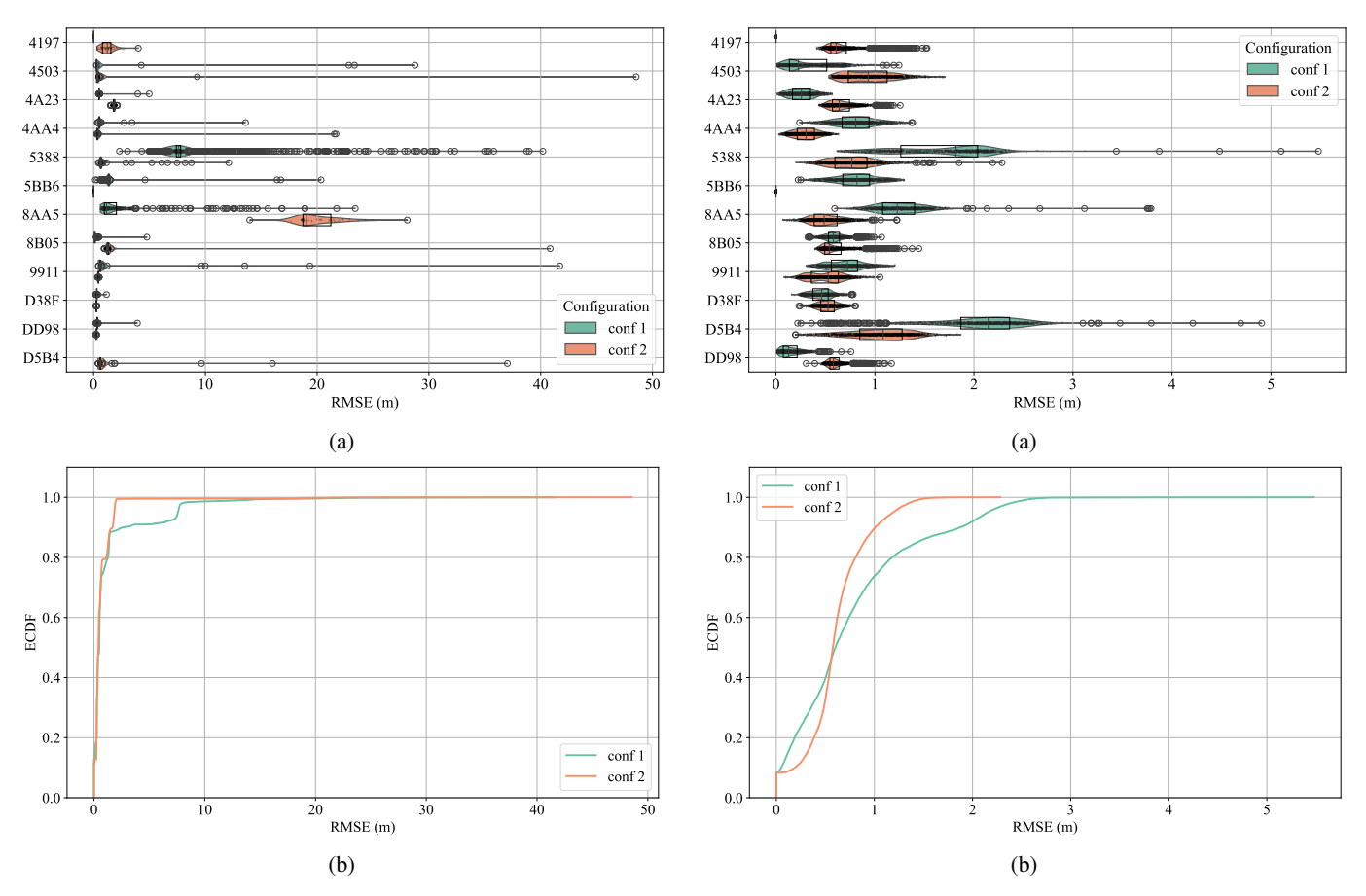


Fig. 12: CF performance analysis: (a) Raincloud plot showing node-wise RMSE across configurations, and (b) RMSE ECDFs. Note the extended RMSE range (0-50 m) indicating substantial positioning failures.

Fig. 13: PGP performance analysis: (a) Raincloud plot showing node-wise RMSE across configurations, and (b) RMSE ECDFs. Note the compressed RMSE range (0-5 m) indicating consistent positioning performance.

substantial configuration sensitivity: Conf. 2 produces broad error distributions with RMSE exceeding $2.2\,\mathrm{m}$ and positioning failures extending to $50\,\mathrm{m}$, while Conf. 1 demonstrates improved consistency with median errors around $0.5\,\mathrm{m}$ and RMSE of $1.3\,\mathrm{m}$. Individual sensors show performance variations, with some nodes transitioning from positioning failure to sub-meter accuracy solely due to anchor reselection.

The PGP method maintains consistent error distributions across configurations, with RMSE values constrained below $5\,\mathrm{m}$ and stable median performance near $0.6\,\mathrm{m}$. The compact probability distributions demonstrate effective decoupling of positioning performance from anchor initialization constraints. These performances differences are also quantified in the ECDFs (Fig. 12b and Fig. 13b).

The PGP method achieves RMSE over all nodes with $0.6\,\mathrm{to}$ $0.8\,\mathrm{m}$ across both configurations. The CF method exhibits configuration-dependent variations: e.g. node 8AA5 has a RMSE difference from $18.23\,\mathrm{m}$ between the configurations.

These performance differences correlate with measurement quality heterogeneity documented in Section V-A. The PGP approach maintains positioning capability by incorporating uncertainty information from multiple anchor hypotheses, processing heavy-tailed ranging distributions without the numerical instabilities that compromise CF trilateration. Nodes

experiencing elevated ranging errors (D5B4, 8AA5) maintain consistent positioning accuracy. The experimental results demonstrate that grid-based uncertainty propagation addresses fundamental limitations in collaborative self-calibration under realistic deployment conditions, maintaining consistent performance across anchor initialization configurations while accommodating mixed-quality measurements.

VI. CONCLUSION

The paper addresses critical limitations in parametric methods that discard spatial uncertainty information when reducing anchor positions to point estimates, particularly problematic in NLOS-contaminated environments. The proposed method implements grid-based uncertainty propagation through discrete Bayesian filtering, maintaining probability distributions across grid cells rather than collapsing to covariance matrices. The weighted likelihood computation preserves distributional information from multiple position hypotheses, enabling robust uncertainty quantification in collaborative networks.

Empirical validation utilized 12 UWB nodes in an industrial environment ($44\,\mathrm{m} \times 30\,\mathrm{m}$), generating 132,000 ranging measurements. Statistical analysis revealed LOS measurements achieved $0.28\,\mathrm{m}$ mean ranging error versus $3.78\,\mathrm{m}$ for NLOS. The grid-based approach demonstrated consistent sub-meter

positioning accuracy across anchor initialization configurations, while baseline CF methods exhibited substantial sensitivity to initialization selection. The experimental results validate that non-parametric uncertainty propagation addresses fundamental limitations in collaborative self-calibration under realistic conditions. The approach maintains positioning capability across varying availability scenarios while accommodating heterogeneous error distributions characteristics.

Future research directions include multi-technology integration combining WiFi, BLE, and 5G within the probabilistic framework for enhanced accuracy and coverage. Hierarchical grid structures and distributed processing architectures could address computational complexity for large-scale deployments. Machine learning integration offers opportunities for automated measurement quality assessment and adaptive state estimation through spatial pattern recognition within likelihood grids. Application domains encompass industrial IoT systems, autonomous navigation platforms, and hybrid positioning networks that leverage reduced infrastructure dependency requirements.

ACKNOWLEDGMENT

The authors acknowledge Deveritec GmbH for providing updated firmware enabling fully meshed measurements and MRK Management Consultants GmbH for facility access.

REFERENCES

REFERENCES

- T. G. Hailu, X. Guo, H. Si, L. Li, and Y. Zhang, "Theories and methods for indoor positioning systems: A comparative analysis, challenges, and prospective measures," in *Sensors*, vol. 24, no. 21. MDPI, 2024, p. 6876
- [2] B. Van Herbruggen, S. Luchie, J. Fontaine, and E. De Poorter, "Multihop self-calibration algorithm for ultra-wideband (uwb) anchor node positioning," *IEEE Journal of Indoor and Seamless Positioning* and Navigation, vol. 1, pp. 1–11, 2023. [Online]. Available: https://ieeexplore.ieee.org/document/10124958
- [3] A. Hossain and W.-S. Soh, "A survey of calibration-free indoor positioning systems," *Computer Communications*, vol. 66, pp. 1–13, 2015.
- [4] K. A. Kordi, M. Roslee, M. Y. Alias, A. Alhammadi, A. Waseem, and A. F. Osman, "Survey of indoor localization based on deep learning," *Computers, Materials & Continua*, vol. 79, no. 2, p. 3261–3298, 2024. [Online]. Available: http://dx.doi.org/10.32604/cmc.2024.044890
- [5] M. Ridolfi, A. Kaya, R. Berkvens, M. Weyn, W. Joseph, and E. D. Poorter, "Self-calibration and Collaborative Localization for UWB Positioning Systems: A Survey and Future Research Directions," ACM Comput. Surv., vol. 54, no. 4, pp. 88:1–88:27, May 2021. [Online]. Available: https://dl.acm.org/doi/10.1145/3448303
- [6] H. Wymeersch, J. Lien, and M. Z. Win, "Cooperative Localization in Wireless Networks," *Proceedings of the IEEE*, vol. 97, no. 2, pp. 427– 450, Feb. 2009, conference Name: Proceedings of the IEEE.
- [7] M. Qi, B. Xue, and W. Wang, "Calibration and Compensation of Anchor Positions for UWB Indoor Localization," *IEEE Sensors Journal*, vol. 24, no. 1, pp. 689–699, Jan. 2024, conference Name: IEEE Sensors Journal. [Online]. Available: https://ieeexplore.ieee.org/document/10325421/?arnumber=10325421
- [8] L. Xu, Z. Li, and X. Li, "A Hybrid Approach Using Multistage Collaborative Calibration for Wireless Sensor Network Localization in 3D Environments," *IEEE Access*, vol. 8, pp. 130 205–130 223, 2020. [Online]. Available: https://ieeexplore.ieee.org/document/9139987/
- [9] K. J. Raja and P. D. Groves, "WiFi-RTT Posterity SLAM for Pedestrian Navigation in Indoor Environments," in ION GNSS+, The International Technical Meeting of the Satellite Division of The Institute of Navigation. Baltimore, Maryland: Institute of Navigation, Oct. 2024, pp. 1864–1877, iSSN: 2331-5954. [Online]. Available: https://www.ion.org/publications/abstract.cfm?articleID=19877

- [10] Y. Lu, O. Kaltiokallio, M. Koivisto, J. Talvitie, E. S. Lohan, H. Wymeersch, and M. Valkama, "Bayesian Filtering for Joint Multi-User Positioning, Synchronization and Anchor State Calibration," *IEEE Transactions on Vehicular Technology*, vol. 72, no. 8, pp. 10 949–10 964, Aug. 2023, conference Name: IEEE Transactions on Vehicular Technology. [Online]. Available: https://ieeexplore.ieee.org/ document/10086654/?arnumber=10086654
- [11] J. Hu, Y. Li, Y. Lei, Z. Xu, M. Lv, and J. Han, "Robust and Adaptive Calibration of UWB-Aided Vision Navigation System for UAVs," *IEEE Robotics and Automation Letters*, vol. 8, no. 12, pp. 8247–8254, Dec. 2023, conference Name: IEEE Robotics and Automation Letters. [Online]. Available: https://ieeexplore.ieee.org/ document/10288387/?arnumber=10288387
- [12] S. Van de Velde, P. Van Torre, and H. Steendam, "Fast and robust anchor calibration in range-based wireless localization," in 2013, 7th International Conference on Signal Processing and Communication Systems (ICSPCS), Dec. 2013, pp. 1–6. [Online]. Available: https: //ieeexplore.ieee.org/document/6723945/?arnumber=6723945
- [13] P. Krapez and M. Munih, "Anchor Calibration for Real-Time-Measurement Localization Systems," *IEEE Transactions on Instrumentation and Measurement*, vol. 69, no. 12, pp. 9907–9917, Dec. 2020. [Online]. Available: https://ieeexplore.ieee.org/document/9127780/
- [14] M. Hamer and R. D'Andrea, "Self-Calibrating Ultra-Wideband Network Supporting Multi-Robot Localization," *IEEE Access*, vol. 6, pp. 22292– 22304, 2018, conference Name: IEEE Access.
- [15] P. Loahavilai, C. Thanapirom, P. Rattanawan, T. Chulapakorn, S. Yan-wicharaporn, C. Kingkan, K. Prasertsuk, and N. Cota, "Rapid Deployment of Ultra-Wideband Indoor Positioning System," in 2021 18th International Joint Conference on Computer Science and Software Engineering (JCSSE), Jun. 2021, pp. 1–6, iSSN: 2642-6579.
- [16] M. Ridolfi, J. Fontaine, B. V. Herbruggen, W. Joseph, J. Hoebeke, and E. D. Poorter, "UWB anchor nodes self-calibration in NLOS conditions: a machine learning and adaptive PHY error correction approach," *Wireless Networks*, vol. 27, no. 4, pp. 3007–3023, May 2021. [Online]. Available: https://link.springer.com/10.1007/s11276-021-02631-0
- [17] D. Medina, L. Grundhofer, and N. Hehenkamp, "Evaluation of estimators for hybrid GNSS-terrestrial localization in collaborative networks," in 2020 IEEE 23rd International Conference on Intelligent Transportation Systems (ITSC). IEEE, Sep. 2020. [Online]. Available: https://doi.org/10.1109/itsc45102.2020.9294750
- [18] A. Jung, P. Schwarzbach, and O. Michler, "Auto-Positioning in Radio-based Localization Systems: A Bayesian Approach," in 2022 IEEE 12th International Conference on Indoor Positioning and Indoor Navigation (IPIN), Sep. 2022, pp. 1–7, iSSN: 2471-917X. [Online]. Available: https://ieeexplore.ieee.org/document/9917513/?arnumber=9917513
- [19] R. G. Brown and P. Y. C. Hwang, Introduction to Random Signals and Applied Kalman Filtering: with MATLAB Exercises, 4th ed. Hoboken, NJ: John Wiley & Sons, 2012.
- [20] L. G. AG, "Leica TS16 Totalstation Einfach vermessen." [Online]. Available: https://leica-geosystems.com/de-de/products/total-stations/robotic-total-stations/leica-ts16